J Mater Sci (2008) 43:3817–3824
DOI 10.1007/s10853-007-2290-6

Coarsening of Co-rich precipitates in a Cu–Co–Fe ternary alloy

Chihiro Watanabe · Daizen Watanabe · Ryoichi Monzen

Received: 6 July 2007 / Accepted: 1 November 2007 / Published online: 13 March 2008

Abstract The effect of coherency on coarsening of fcc Co–Fe precipitates in a Cu–1.47 wt.%Co–0.56 wt.%Fe (Co : Fe = 7:3 in atomic ratio) alloy aged at 873–973 K has been studied by measuring both the precipitate size by transmission electron microscopy and the solute concentration in the Cu matrix by electrical resistivity measurements. The precipitate phase consists of 7 parts of Co and 3 parts of Fe in atomic ratio, irrespective of the precipitate size. The precipitates smaller than about 8 nm in radius are coherent with the Cu-matrix. When the average precipitate radius is over 18 nm, all the precipitates become semi-coherent. The coarsening rates are not affected by the coherency of the precipitates. The precipitate/matrix interface energy γ has been derived, independently of the diffusivities of solute atoms using a coarsening model developed by Kuehmann and Voorhees for ternary systems. The precipitates are coherent or semi-coherent with the matrix, the experimentally obtained value of γ is 0.2 J/m^2. This value lies between the reported values of $\gamma = 0.15$ J/m^2 for Co precipitates and $\gamma = 0.25$ J/m^2 for γ-Fe precipitates.

Introduction

Coarsening or Ostwald ripening is defined as the microstructural change occurring during the late stages in precipitation reaction. The simplest change is that the average size of second phase precipitates increases with aging time at a virtually constant volume fraction. This results in the growth of precipitates larger than a certain critical size and the shrinkage of precipitates smaller than the critical size. The first quantitative theory for coarsening in binary systems was by Lifshitz and Slyozov [1] and Wagner [2], and is generally called the LSW theory. Although the original LSW theory was developed for binary systems, this analysis has subsequently been extended to multicomponent systems [3–5]. Recently, Kuehmann and Voorhees (KV) [6] developed a coarsening model for ternary system, which includes the effects of capillarity on the precipitate composition and predicts that coarsening behavior of second phase depends strongly on the partitioning behavior and the diffusivities of the alloying elements. Using the KV model, several experimental studies of coarsening kinetics of intermetallic (order-phase) precipitates in ternary system alloys have been conducted [7–11]. However, the coarsening of disordered-phase precipitates in ternary systems has not been examined yet.

We have examined the coarsening behavior of fcc Co precipitates in a Cu–1 wt.%Co alloy during aging at 873, 923, 973, and 998 K [12]. The transmission electron microscopy (TEM) work showed that the average radius at which the transition occurred from a coherent to a semi-coherent interface was about 6 nm. The Cu/Co interface energy γ and diffusion coefficient D of Co in the Cu matrix were derived independently from data on coarsening alone using the LSW theory. The experimentally obtained value of $\gamma = 0.15$ J/m^2 was insensitive to the coherency change. Also Monzen and Kita [13] have investigated the coarsening of γ-Fe precipitates in a Cu–1.7 wt.%Fe alloy by means of TEM observations and resistivity measurements. Applying the LSW theory for the experimental data, the independent value of $\gamma = 0.25$ J/m^2 was estimated.

C. Watanabe (✉) · D. Watanabe · R. Monzen
Division of Innovative Technology and Science, Kanazawa University, Kakuma-machi, Kanazawa 920–1192, Japan
e-mail: chihiro@t.kanazawa-u.ac.jp

However, the effect of change in coherency of the γ-Fe precipitates on the interface energy was not studied.

Using the lattice constants of 0.3615 nm for Cu [14], 0.3548 nm for fcc Co [15], and 0.3562 nm for γ-Fe [16], the lattice misfit between Cu and fcc Co or γ-Fe is calculated as -0.019 or -0.015. Aging of Cu-base alloys containing Co and Fe produces disordered fcc Co–Fe precipitates [17–19]. The lattice misfits between the Cu matrix and the precipitates can be continuously changed by varying the amounts of Co and Fe in alloys.

In this study, we examine the coarsening of Co–Fe precipitates in a Cu–1.47 wt.%Co–0.56 wt.%Fe alloy aged at 873–973 K, focusing on (i) effects of coherency of the Cu matrix/precipitate interface on the coarsening behavior and (ii) estimation of the independent values of γ using the KV model. Observations by TEM and electrical resistivity measurements were performed in order to describe the microstructural evolution and concentration of solute atoms in the Cu matrix. This research is part of a comprehensive study of coarsening behavior of the Co–Fe precipitates in Cu–Co–Fe ternary alloys which have various compositions.

Experimental procedure

Cu–1.47 wt.%Co–0.56 wt.%Fe ingots were prepared in a melting furnace under an Ar atmosphere. The atomic ratio of Co/Fe for this alloy is 7:3. The alloy was cut into strips with a thickness of 10 mm. The strips were cold-rolled to a thickness of 1 mm. Specimens were then homogenized at 1,323 K for 5 h to produce a solid solution, and quenched into cold water. The solution-treated specimens were aged in a vacuum at 873, 923, and 973 K for various periods. After the desired aging times were reached, they were quenched into cold water.

Three millimeter diameter disks were punched from the aged foils, mechanically ground down to 200 μm, and electro-polished using a solution of 20% phosphoric acid at 273 K. Microscopy was performed using a JEOL 2000EX and a 2010FEF microscope at an operation voltage of 200 kV. The average radius of precipitates was measured from high-resolution and bright-field TEM images of the precipitates. The precipitate coherency was judged from the Ashby and Brown [20, 21] contrast which appears around a spherical coherent precipitate in bright-field images. The details of the principle and process for the judgment of precipitate coherency are described in the literature [22]. To obtain statistically reliable data, more than 200 precipitates were analyzed for each aging condition. In order to obtain the composition of the precipitate phase, TEM foils were examined in a JEOL 2010FEF microscope operated at 200 kV and equipped with an energy dispersive X-ray spectroscopy system.

The specimens for electrical resistivity measurements were cut to the size of 200 × 12 × 0.3 mm^3. After aging, resistivity measurements were made at room temperature (293 K) using a standard four-point potentiometric technique. The measurements were repeated ten times to obtain one data point, reversing the current direction to eliminate the stray electromotive force. The cross-sectional area of specimens was measured at different positions and the average value was evaluated.

Results and discussion

Precipitate phase

Figure 1a–c show the microstructure of the present alloy aged at 700 °C. The insets at lower right in Fig. 1a–c are selected-area diffraction patterns (SADPs) taken from the areas containing Co–Fe precipitates. Extensive analyses of the SADPs revealed that the precipitate phase has a disordered fcc structure.

An energy-dispersive X-ray (EDX) analysis of the Co–Fe precipitates was performed to obtain the chemical composition of the precipitates in the specimen aged at 700 °C for 10 min, 50 h, and 334 h. The average precipitate radii are 6, 35, and 75 nm in these aging conditions, respectively. Figure 2 presents the concentrations of Co and Fe plotted as a function of Cu concentration. A linear relationship can be seen between the concentrations of Cu and Co or Fe. Although the EDX analysis was carried out using the beam directed at the Co–Fe precipitates, Cu atoms were always detected, as seen in Fig. 2. Thus, in order to exclude the influence of Cu, from the intercepts of the straight lines drawn by the least-squares method, the concentrations of Co and Fe in the precipitates were obtained as 0.69 and 0.31, respectively. That is, the composition of the precipitates is about 70%Co–30%Fe in atomic fraction, independent of the size of precipitates. This ratio is consistent with the ratio of atomic amounts of Co and Fe in the present alloy.

Coarsening of precipitates

As depicted in Fig. 1, the size of the precipitates increases and the number density of the precipitate decreases as the aging time increases. Small Co–Fe precipitates were nearly spherical and coherent with the Cu matrix, as shown in Fig. 1a. However, the Ashby and Brown contrasts became irregular, when the precipitate radius was over about 8 nm. This indicates that the interface between the precipitate and Cu matrix became semi-coherent with precipitate growth. Semi-coherent precipitates larger than about 20 nm in

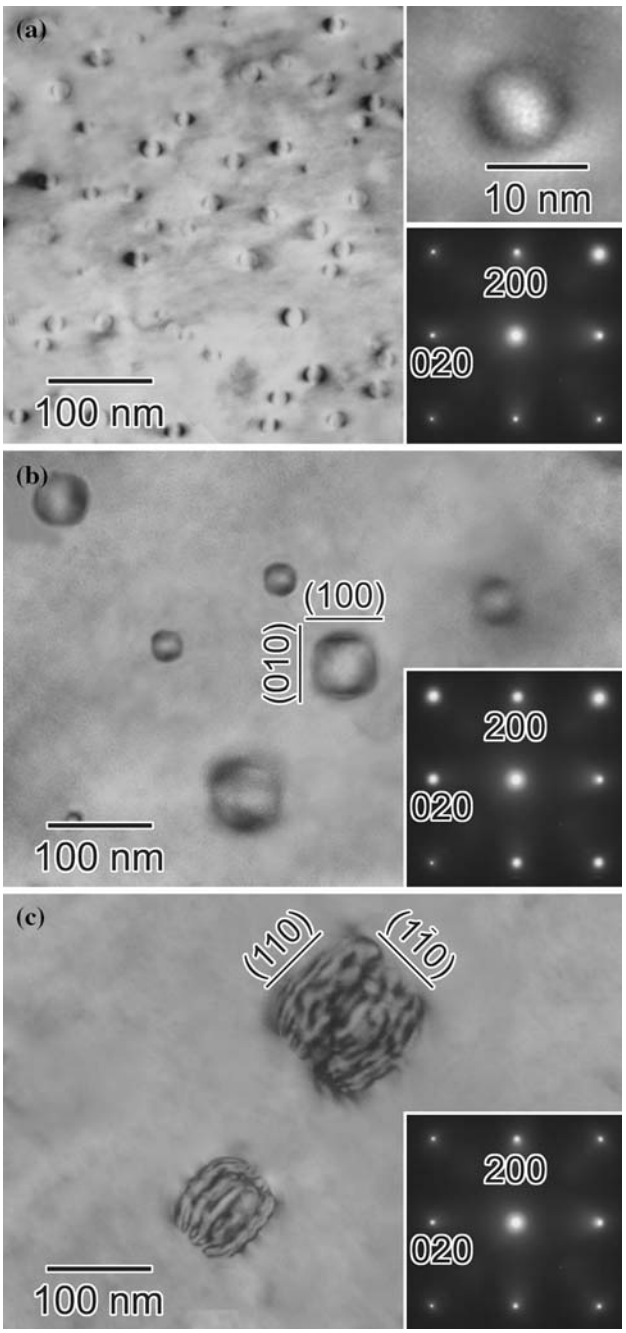

Fig. 1 Bright-field images of fcc Co–Fe precipitates in a Cu–1.47 wt.%Co–0.56 wt.%Fe alloy aged at 973 K for (**a**) 10 min, (**b**) 9 h and (**c**) 150 h. The inset at upper right in (**a**) is a magnified exact-axis bright-field image of a precipitate

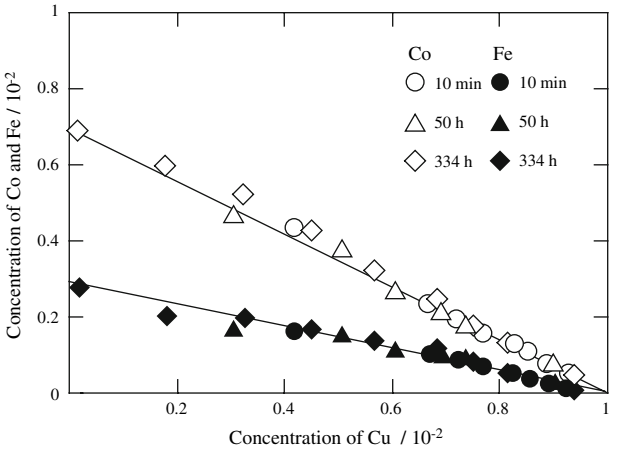

Fig. 2 Results of EDX analysis obtained from Co–Fe precipitates in a Cu–1.47 wt.%Co–0.56 wt.%Fe alloy aged at 973 K for 10 min, 9 h, and 150 h

radius tended to become a nearly cuboidal shape with flat interfaces parallel to {100}, as clearly recognized in Fig. 1b. These nearly cuboidal precipitates have been reported in an aged Cu–Co–Cr alloy [23] and a Cu–Co alloy [12]. Moreover, when the precipitate radius was larger than about 40 nm, they tended to become octahedral with {111} habit planes. These observations are consistent with previous work [12, 24]. The nearly cuboidal or octahedral shape is assumed to be a supersphere, and the supersphere is reduced to a sphere which has the same volume as the supersphere [25, 26].

The coherency of the matrix/precipitate interfaces was judged from the Ashby-Brown contrast in bright-field images. Figure 3 shows the ratio of semi-coherent precipitates to the total number of precipitates at each average radius. For comparison, the result of a Cu–1 wt.%Co binary alloy obtained previously [12] is also indicated in Fig. 3. The ratio rapidly increases from about 8 nm to 18 nm, and no clear dependence on aging temperature and time was observed. Similar to our previous work [9, 12], the precipitation process can be divided into three stages: (1) coherent stage ($r < 8$ nm), with almost all precipitates coherent, (2) intermediate stage ($8 < r < 18$ nm), with coexisting coherent and semi-coherent precipitates and (3) semi-coherent stage ($r > 18$ nm), with almost all precipitates semi-coherent. It should be noted, however, that the critical radius for coherent/semi-coherent transition of the precipitates in the present ternary alloy is larger than that ($6 < r < 12$ nm) for the Cu–Co binary alloy. This can be understood because the lattice parameter of fcc Co is smaller than that of Cu and the solute Fe in Co makes the lattice parameter slightly larger [27].

In the KV mathematical treatment of coarsening [6], the time dependence of the average precipitate radius r is described by

$$r^n - r_0^n = K(t - t_0), \tag{1}$$

where $n = 3$ is the predicted exponent, r_0 is the average radius of precipitates at the onset of coarsening at time t_0 and K is the rate constant which is dependent on the interfacial energy and diffusion coefficients of Co and Fe in

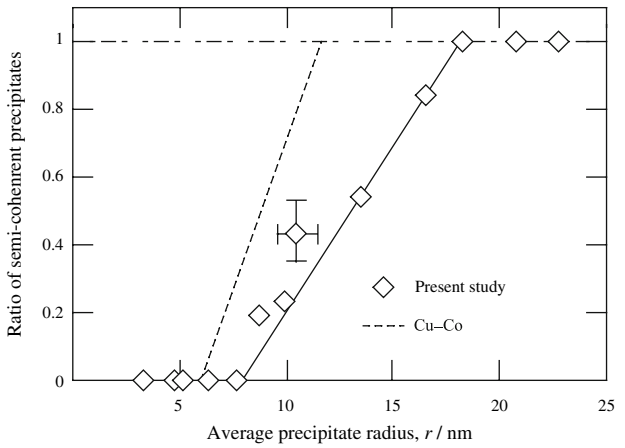

Fig. 3 Ratio of semi-coherent Co–Fe precipitates to the total number of Co–Fe precipitates in a Cu–1.47 wt.%Co–0.56 wt.%Fe alloy aged at 873, 923 and 973 K. Also shown is the result for a Cu–1 wt.%Co alloy obtained by Watanabe et al. [12]

Cu. Eq. (1) exhibits the same time dependence for both binary and ternary systems, but the K is significantly different and given by the equation

$$K = \frac{8\gamma V_m}{9\Lambda}. \tag{2}$$

Here, γ is the interface energy between the precipitate phase and Cu matrix and V_m is the atomic volume per mol of the precipitates, calculated from $V_m = N_a a^3/4$, where N_a is Avogadro's number and a is the lattice constant of the precipitate phase (= 0.3552 nm). The coefficient Λ is given as

$$\Lambda = \frac{\Delta c_{\mathrm{Co}}}{D_{\mathrm{Co}}}\left(\Delta c_{\mathrm{Co}} G''_{\mathrm{CoCo}} + \Delta c_{\mathrm{Fe}} G''_{\mathrm{CoFe}}\right) + \frac{\Delta c_{\mathrm{Fe}}}{D_{\mathrm{Fe}}}\left(\Delta c_{\mathrm{Co}} G''_{\mathrm{CoFe}} + \Delta c_{\mathrm{Fe}} G''_{\mathrm{FeFe}}\right), \tag{3}$$

where $\Delta c_{\mathrm{i}} = c_{\mathrm{i}}^{\mathrm{P}} - c_{\mathrm{i}}^{\mathrm{M}}$; $c_{\mathrm{i}}^{\mathrm{P/M}}$ is the concentration of the i-th element in the precipitate and matrix near the precipitate interface. During coarsening, the system is very close to equilibrium. This allows us to assume an approximation that $\Delta c_{\mathrm{i}} = c_{\mathrm{i}}^{\mathrm{P}} - c_{\mathrm{i}}^{\mathrm{M}} \approx c_{\mathrm{i}}^{\mathrm{P}}(\infty) - c_{\mathrm{i}}^{\mathrm{M}}(\infty)$, where $c_{\mathrm{i}}^{\mathrm{P/M}}(\infty)$ is the concentration far from the Cu/precipitate interfaces. The D_{Co}or D_{Fe} is the diffusion coefficient of Co or Fe in the Cu matrix. The $G'_{\mathrm{pq}}{}'$ are the second derivatives of the Gibbs free energy with respect to the concentration of p and q, with p, q = Co, Fe.

Log–log plots of r versus t yield slopes of $1/n$. Figure 4 displays the average precipitate radius r against aging time t on logarithmic scales. The experimental slopes are nearly identical to the value 1/3 excepting at early times. Figure 5 shows the coarsening curves of the Co-rich precipitates in the present ternary alloy aged at 873, 923 and 973 K. A linear relationship exists between r^3 and t, except for the early stage of aging. As shown in the upper right of Fig. 5, the growth rate decreases gradually and reaches a constant value above about 7×10^4, 4×10^3 and 1×10^3 s at 873, 923 and 973 K respectively. The cause of the growth rate change will be discussed later. Experimental values of K were determined from the slopes of the straight lines using experimental points above these times in Fig. 5, and Table 1 lists the values of K, along with the reported values for a Cu–Co [12] and a Cu–Fe alloy [13]. The values of K for the present ternary alloy are larger than those for the Cu–Co binary alloy and smaller than those for the Cu–Fe binary alloy aged at 923 and 973 K.

Change in solute concentration in Cu matrix

The KV model of coarsening for a ternary alloy predicts that the concentration C_i with i = Co or Fe in Cu matrix after coarsening time t varies as [6]

$$C_{\mathrm{i}} - C_{\mathrm{i,e}} = k_{\mathrm{i}} t^{-1/3}, \tag{4}$$

where $C_{i,e}$ is the solid-solubility of i component in the Cu matrix and k_{i} is a coarsening parameter given by

$$k_{\mathrm{i}} = \frac{(3\gamma V_{\mathrm{m}})^{2/3}\Lambda^{1/3}\Delta c_{\mathrm{i}}}{\Delta c_{\mathrm{Co}}\left(\Delta c_{\mathrm{Co}} G''_{\mathrm{CoCo}} + \Delta c_{\mathrm{Fe}} G''_{\mathrm{CoFe}}\right) + \Delta c_{\mathrm{Fe}}\left(\Delta c_{\mathrm{FeFe}} G''_{\mathrm{FeFe}} + \Delta c_{\mathrm{Co}} G''_{\mathrm{CoFe}}\right)}. \tag{5}$$

As noticed above, the composition of the precipitates is 7 parts of Co and 3 of Fe in atomic fraction, and essentially independent of the precipitate size examined in this study. Thus, values of C_{i} were determined by applying the values of electrical resistivity to the experimental data regarding the dependence of electrical resistivity on Co and Fe concentration [28], taking the ratio of Co/Fe into account.

Following Eq. (4), plots of C_{i} against $t^{-1/3}$ are shown in Fig. 6. Hereafter, the concentration will be represented as an atomic fraction. For each aging temperature, C_{i} exhibits a steep decrease and, over a time, a linear relationship is observed between C_{i} and $t^{-1/3}$. Table 2 lists the values of k_{i} obtained from the slopes of the straight lines, determined by the least-squares method, and the values of

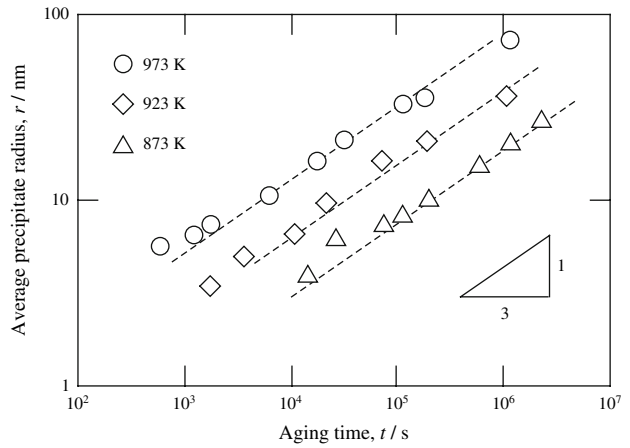

Fig. 4 Variation in the average precipitate radius r with aging time t for a Cu–1.47 wt.%Co–0.56 wt.%Fe alloy aged at 873, 923, and 973 K. Dashed lines with slope = 1/3 are superimposed

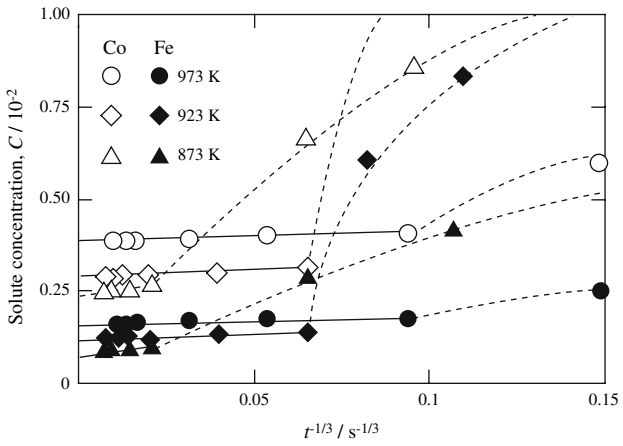

Fig. 6 Variation in the solute concentration C of the matrix of a Cu–1.47 wt.%Co–0.56 wt.%Fe alloy aged at 873, 923 and 973 K as a function of $t^{-1/3}$

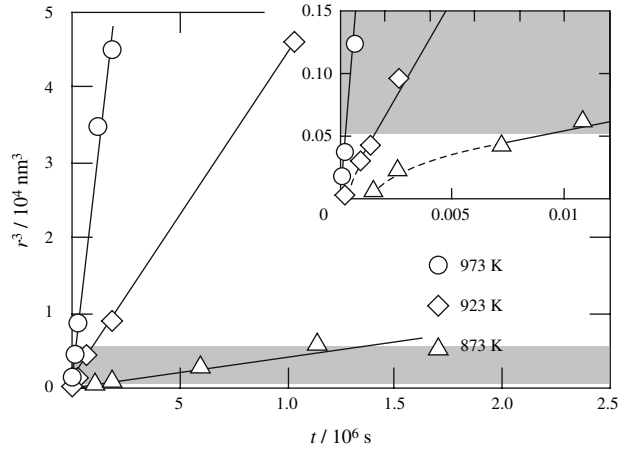

Fig. 5 Coarsening plot of Co–Fe precipitates in a Cu–1.47 wt.%Co–0.56 wt.%Fe alloy aged at 873, 923, and 973 K. The shaded area indicates the intermediate stage ($8 < r < 18$ nm) where coherent and semi-coherent Co–Fe precipitates coexist

Table 1 Values of the coarsening rate constant K for Cu–1.47 wt%Co–0.56 wt%Fe, Cu–1 wt.%Co [12] and Cu–1.7 wt.%Fe alloys [13]

T(K)	$K/10^{-30}$(m^3 s^{-1})		
	Present study	Cu–Co	Cu–Fe
873	8.80 ± 0.15	3.47	6.44
923	45.0 ± 6.1	18.5	60.1
973	263 ± 15.0	65.0	379

$C_{i,e}$, obtained directly by extrapolation to $t^{-1/3} = 0$. The reported values of solubility for a Cu–Co [12] and a Cu–Fe alloy [13] are also shown in Table 2. The obtained values of $C_{Co,e}$ and $C_{Fe,e}$ in the present ternary alloy are smaller than the reported values of solubility of Co and Fe in Cu. The calculated Cu–Co–Fe ternary equilibrium diagrams [29] show that Co and Fe dissolving simultaneously into Cu reduce slightly the solubility of both Co and Fe in Cu. Although the ternary equilibrium diagrams were calculated for higher temperatures than the aging temperatures examined in this study, the smaller values of C_e in this work may be reasonably accepted.

The volume fraction f of precipitates was determined by applying the values of electrical resistivity, before and after aging, to the linear relationships between the electrical resistivity and concentration of Co or Fe in Cu. Figure 7 depicts the calculated values of f as a function of t, together with the precipitate number density $N = 3f/(4\pi\ r^3)$. For each aging temperature, f shows first a rapid increase and, over a time, a nearly linear relationship exists between f and log t. The linear relationship is observed after about 7.2×10^4 s at 873 K, 3.6×10^3 s at 923 K and 1.2×10^3 s at 973 K. These times are identical to those above which, in Fig. 5, the kinetics of the decay of supersaturation with t on aging at the temperatures obey the prediction of the KV model. Therefore, the coarsening of the precipitates begins over about 7.2×10^4 s at 873 K, 3.6×10^3 s at 923 K, and 1.2×10^3 s at 973 K. On the other hand, N keeps falling and the slopes show the expected theoretical value of -1 for precipitate coarsening in ternary systems [6]. These results indicate that the growth and coarsening take place simultaneously before the coarsening starts. In this mixed stage of growth and coarsening, supersaturated solute atoms in the Cu matrix tend to be captured by the precipitates. This may explain the faster growth of the precipitates in the mixed stage. Therefore, the change in growth rate in Fig. 5 is attributable to the transition from the growth and coarsening stage to the coarsening stage.

Table 2 Values of the coarsening parameter $k^{-1/3}$ for Cu–1.47 wt.%–0.56 wt.%Fe alloy, and values of the solubility C_e of Co and Fe in the Cu matrix for Cu–1.47 wt.%Co–0.56 wt.%Fe, Cu–1 wt.%Co [12], and Cu–1.7 wt.%Fe alloys [13]

T(K)	$k_{Co}/10^{-3}(s^{1/3})$	$k_{Fe}/10^{-3}(s^{1/3})$	C_e(wt.%)			
			CO		γ-Fe	
			Present study	Cu–Co	Present study	Cu–Fe
873	4.78 ± 0.35	2.05 ± 0.35	0.23 ± 0.01	0.45	0.094 ± 0.005	0.17
923	3.02 ± 0.50	1.29 ± 0.50	0.27 ± 0.01	0.53	0.11 ± 0.01	0.28
973	2.19 ± 0.34	0.94 ± 0.34	0.36 ± 0.01	0.60	0.15 ± 0.01	0.50

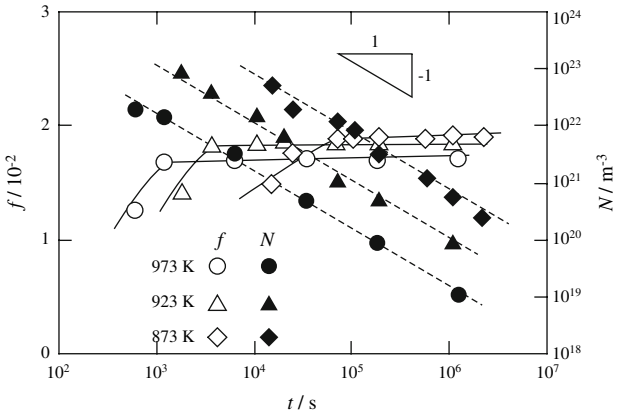

Fig. 7 Variation in the volume fraction f and the number density N of Co–Fe precipitates in a Cu–1.47 wt.%Co–0.56 wt.%Fe alloy aged at 873, 923, and 973 K. Dashed lines with slope = −1 are superimposed

Calculation of γ

Using the subregular solution model, we have

$$G''_{CoCo} = RT\left(\frac{1}{c^M_{Co}(\infty)} + \frac{1}{1 - c^M_{Co}(\infty) - c^M_{Fe}(\infty)}\right) - 2L_{CuCo} - 2L_{CuCoFe}c^M_{Fe}(\infty), \quad (6)$$

$$G''_{CoFe} = \frac{RT}{1 - c^M_{Co}(\infty) - c^M_{Fe}(\infty)} - L_{CuCo} + L_{CoFe} - L_{FeCu} + L_{CuCoFe}\left(1 - 2c^M_{Co}(\infty) - 2c^M_{Fe}(\infty)\right), \quad (7)$$

$$G''_{FeFe} = RT\left(\frac{1}{1 - c^M_{Co}(\infty) - c^M_{Fe}(\infty)} + \frac{1}{c^M_{Fe}(\infty)}\right) - 2L_{FeCu} - 2L_{CuCoFe}c^M_{Co}(\infty), \quad (8)$$

where RT has its usual meaning, L_{ij} is the interaction parameter between i and j atoms, and L_{CuCoFe} is the ternary interaction parameter. The data on L_{CuCo}, L_{FeCu}, L_{CoFe}, and L_{CuCoFe} have been reported in literature [27, 29–31] and are calculated to be 38, 46, −9, and −28 kJ mol^{-1} for the present alloy, respectively. For the later stage of aging where the precipitation reaction is complete and only coarsening of the precipitates is taking place, $c^M_{Co}(\infty)$ and $c^M_{Fe}(\infty)$ will be approximately equal to $C_{Co,e}$ and $C_{Fe,e}$, respectively. In addition, the solute concentration in the Cu matrix is negligibly small compared to that in the precipitate phase at any time (Fig. 6), and we now obtain $\Delta c_{Co} \approx 0.7$ and $\Delta c_{Fe} \approx 0.3$.

Combination of the K and k_i enables the matrix / precipitate interface energy γ to be calculated without having to assume the values of D_{Co} and D_{Fe}:

$$\gamma = \frac{K^{1/3}}{2V_m}\frac{k_i}{\Delta c_i}\left[\Delta c_{Co}\left(\Delta c_{Co}G''_{CoCo} + \Delta c_{Fe}G''_{CoFe}\right) + \Delta c_{Fe}\left(\Delta c_{Fe}G''_{FeFe} + \Delta c_{Co}G''_{CoFe}\right)\right]. \quad (9)$$

The values of γ calculated from Eq. (9) are listed in Table 3. The value of γ is about 0.2 J/m^2. The change in growth rate corresponding to the transition from the coherent stage to intermediate stage or the intermediate stage to the semi-coherent stage is not detected in the growth curves on aging at 873, 923, and 973 K in Fig. 5. It can thus be stated that the experimentally obtained value of $\gamma \approx 0.2$ J/m^2 by the KV model is insensitive to the coherency of the precipitate/Cu matrix interfaces. However, it is generally accepted that the transition from a coherent interface to a semi-coherent interface results in an increase in the interface energy [32, 33]. This discrepancy can be explained by free energy analyses for the coarsening of coherent and semi-coherent precipitates, as will be reported in details in a separate paper [34]. The obtained value of $\gamma \approx 0.2$ J/m^2 lies between the

Table 3 Values of the interface energy γ calculated for Cu–1.47 wt.%Co–0.56 wt.%Fe, Cu–1 wt.%Co [12], and Cu–1.7 wt.%Fe alloys [13]

T(K)	γ(Jm^{-2})		
	Present study	Cu–Co	Cu–Fe
873	0.200 ± 0.020	0.149	0.24
923	0.196 ± 0.028	0.148	0.27
973	0.199 ± 0.025	0.151	0.25

reported values of $\gamma \approx 0.15$ J/m^2 for a Cu–Co binary alloy [12] and $\gamma \approx 0.25$ J/m^2 for a Cu–Fe binary alloy [13]. We feel that the reliability of this value is high in terms of the technique employed, which have not needed to assume values of diffusivity and solubility of solute atoms.

Direct application of the KV model has been directed at some ternary system alloys [4, 5, 7] to estimate the value of γ. In that case, the ideal solution theory was adopted, since interaction parameters between solute and solvent atoms are often uncertain. Assuming that the Cu matrix is described by the dilute ideal-solution theory, the G''_{pq} can be rewritten as

$$G''_{CoCo} = RT\left(\frac{1}{c^{M}_{Co}(\infty)} + \frac{1}{1 - c^{M}_{Co}(\infty) - c^{M}_{Fe}(\infty)}\right), \quad (10)$$

$$G''_{CoFe} = \frac{RT}{1 - c^{M}_{Co}(\infty) - c^{M}_{Fe}(\infty)}, \quad (11)$$

$$G''_{FeFe} = RT\left(\frac{1}{1 - c^{M}_{Co}(\infty) - c^{M}_{Fe}(\infty)} + \frac{1}{c^{M}_{Fe}(\infty)}\right). \quad (12)$$

In these G_{pq}'' deduced using the ideal-solution theory, the interaction terms in Eqs. 6–8 are totally neglected. Values of γ were recalculated from Eq. 9 using Eqs. 10–12. The average value of γ was about 0.22 J/m^2, which is slightly larger than that of 0.2 J/m^2 obtained using the complex subregular solution model. Therefore, the value of γ can be roughly estimated by adopting the simple ideal-solution theory even if the interaction parameters for a system are uncertain.

Calculation of D

By combining (2), (3), and (5), we have a relation of

$$\frac{k_{Co}}{\Delta c_{Co}} = \frac{k_{Fe}}{\Delta c_{Fe}}.$$

This relation does not permit us to calculate independent values of D_{Co} and D_{Fe} from coarsening data alone. From Eqs. 2, 3, and 9, D_{Co} and D_{Fe} are deduced as

$$D_{Co} = \frac{9K^{2/3}(\Delta c_{Co})^2 D_{Fe}\left(\Delta c_{Co}G''_{CoCo} + \Delta c_{Fe}G''_{CoFe}\right)}{4k_{Co}D_{Fe}\left(\Delta c_{Co}\left(\Delta c_{Co}G''_{CoCo} + \Delta c_{Fe}G''_{CoFe}\right) + \Delta c_{Fe}\left(\Delta c_{Co}G''_{CoFe} + \Delta c_{Fe}G''_{FeFe}\right)\right) - 9K^{2/3}\Delta c_{Co}\Delta c_{Fe}\left(\Delta c_{Co}G''_{CoFe} + \Delta c_{Fe}G''_{FeFe}\right)} \quad (13)$$

and

$$D_{Fe} = \frac{9K^{2/3}\Delta c_{Co}\Delta c_{Fe}D_{Co}\left(\Delta c_{Co}G''_{CoFe} + \Delta c_{Fe}G''_{FeFe}\right)}{4k_{Co}D_{Co}\left(\Delta c_{Co}\left(\Delta c_{Co}G''_{CoCo} + \Delta c_{Fe}G''_{CoFe}\right) + \Delta c_{Fe}\left(\Delta c_{Co}G''_{CoFe} + \Delta c_{Fe}G''_{FeFe}\right)\right) - 9K^{2/3}(\Delta c_{Co})^2\left(\Delta c_{Co}G''_{CoCo} + \Delta c_{Fe}G''_{CoFe}\right)}. \quad (14)$$

From these equations, it is noted that the diffusivity of a solute atom is yielded as a function of the diffusivity of another, and thus cannot be calculated independently of one another. Values of D_{Co} and D_{Fe} were then calculated from Eqs. 13 and 14 using reported impurity diffusion data for Fe [14] and Co [35] in Cu. Figure 8 presents the plots of D_{Co} and D_{Fe} obtained as a function of T^{-1}, together with the reported diffusion data for Co and Fe in Cu. It is seen in Fig. 8 that the present data are consistent with the impurity diffusion data for Co and Fe in Cu. Although there are only three data points, the pre-exponential factor D_0 and the activation energy Q can be determined from the intercept and slope of the straight lines fitted to the D data. The estimated values of D_0 and Q were 1.0×10^{-4} m^2 s^{-1} and 216 kJ mol^{-1} for Co, and 1.2×10^{-4} m^2 s^{-1} and 215 kJ mol^{-1} for Fe, which agree well with the reported values for impurity diffusion of Co and Fe in Cu.

Conclusions

The coarsening of precipitates in a Cu–1.47 wt%Co–0.56wt%Fe alloy during aging at 873, 923, and 973 K has been examined using the Kuehmann and Voorhees (KV) model [6] by combined techniques of TEM observations and electrical resistivity measurements. The results and conclusions are summarized as follows:

(1) Aging of the alloy produces fcc Co–Fe precipitates, consisting of 7 parts of Co and 3 of Fe in atomic fraction, regardless of the precipitate size.
(2) The precipitates smaller than 8 nm in radius are coherent with the Cu-matrix. When the average precipitate radius is larger than 18 nm, all the precipitates become semi-coherent. The ratio of the semi-coherent precipitates rapidly increases from 8 nm to 18 nm.
(3) The average radius of the precipitates increases with aging time t as $t^{1/3}$, as predicted by the KV model.

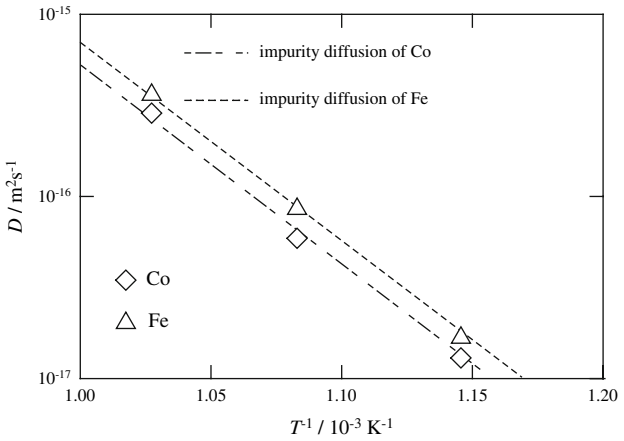

Fig. 8 Comparison of the diffusivity values obtained in the present study with impurity diffusion data for Co [35] and Fe [14] available in the literature

The kinetics of the decay of supersaturation with t follow the predicted $t^{-1/3}$ law.

(4) Independent value of the matrix/precipitate interface energy γ has been successfully obtained from application of the KV model. The experimentally obtained value of γ is about 0.2 J/m^2. This value is higher than the reported value of $\gamma = 0.15$ J/m^2 [12] for Co precipitates in Cu matrix, but lower than that of $\gamma = 0.25$ J/m^2 [13] for γ-Fe precipitates.

(5) The diffusivities D of Co and Fe in the Cu matrix have been derived from the KV model using data on coarsening. The estimates of D are nearly identical to reported impurity diffusion data for Co [35] and Fe [14] in Cu.

Acknowledgements This work has been partially supported by Inoue Foundation for Science. The authors thank Professor K. Tazaki, Kanazawa University, for use of the JEOL 2000EX and 2010FEF. We also acknowledge Mr. K. Higashimine of the Center for Nano Materials and Technology, Japan Advanced Institute of Science and Technology, for the TEM observations.

References

1. Lifshitz IM, Slyozov VV (1961) J Phys Chem Solids 19:35
2. Wagner C (1961) Z Elektrochem 65:581
3. Bhattacharyya SK, Russell KC (1972) Metall Trans 3:2195
4. Bhattacharyya SK, Russell KC (1976) Metall Trans A 7:453
5. Lee HM, Allen SM, Grujicic M (1991) Metall Trans A 22:2863
6. Kuehmann CJ, Voorhees PW (1996) Metall Mater Trans A 27:937
7. Marquis EA, Seidman DN (2005) Acta Mater 53:4259
8. Fuller CB, Seidman DN (2005) Acta Mater 53:5415
9. Watanabe C, Watanabe D, Monzen R (2006) Mater Trans 47:2285
10. Sudbrack CK, Yoon KE, Noebe RD, Seidman DN (2006) Acta Mater 54:3199
11. Watanabe D, Watanabe C, Monzen R (2007) Mater Trans 48:1571
12. Watanabe D, Higashi K, Watanabe C, Monzen R (2006) J Japan Inst Metals 71:151
13. Monzen R, Kita K (2002) Philos Mag Lett 82:373
14. Japan Institute of Metals (2004) Kinzoku data book. Maruzen, Tokyo, p 37
15. Heinrich B, Cocharan JF, Kowalewski M, Kirshner J, Celinski Z, Arrott AS, Myrtle K (1991) Phys Rev B 44:9348
16. Kato M, Monzen R, Mori T (1978) Acta Metall 26:605
17. Monzen R, Kato M (1992) J Mater Sci Lett 11:56
18. Lin M, Olson GB, Cohen M (1993) Acta Metall Mater 41:253
19. Fujii T, Kato T, Yamada T, Kato M, Nimori S, Ohtsuka H (2003) Mater Trans 44:2545
20. Ashby MF, Brown LM (1963) Philos Mag 8:1083
21. Ashby MF, Brown LM (1963) Philos Mag 8:1649
22. Iwamura S, Miura Y (2004) Acta Mater 52:591
23. Fujii T, Tamura T, Kato M, Onaka S (2002) Microsc Microanal 8:1434
24. Satoh S, Johnson WC (1992) Metall Trans A 23:2761
25. Onaka S, Kobayashi N, Fujii T, Kato M (2003) Mater Sci Eng A 347:42
26. Onaka S, Fujii T, Kato M (2005) Mech Mater 37:179
27. Ohnuma I, Enoki H, Ikeda O, Kainuma R, Ohtani H, Sundman B, Ishida K (2002) Acta Mater 50:379
28. Linde JO (1968) Helv Phys Acta 41:1007
29. Wang CP, Liu XJ, Ohnuma I, Kainuma R, Ishida K (2002) J Phase Equilib 23:236
30. Palumbo M, Curiotto S, Battezzati L (2006) Calphad 30:171
31. Turchanin MA, Agraval PG, Nikolaenko IV (2003) J Phase Equilib 24:307
32. Turnbull D (1955) Impurities and interfaces. ASM, Metals Park, p 121
33. Jesser WA (1969) Phil Mag 19:993
34. Watanabe D, Watanabe C, Monzen R (2007) J Mater Sci. doi:10.1007/s10853-007-2373-4
35. Dohl R, Macht M-P, Naundorf V (1984) Phys Stat Sol (a) 86:603